

# Human Tactile Gesture Interpretation for Robotic Systems

Elizabeth “Bibit” Bianchini, Kenneth Salisbury, and Prateek Verma

**Abstract**—Human-robot interactions are less efficient and communicative than human-to-human interactions, and a key reason is a lack of informed sense of touch in robotic systems. Existing literature demonstrates robot success in executing handovers with humans, albeit with substantial reliance on external sensing or with primitive signal processing methods, deficient compared to the rich set of information humans can detect. In contrast, we present models capable of distinguishing between four classes of human tactile gestures at a robot’s end effector, using only a non-located six-axis force sensor at the wrist. Due to the absence in the literature, this work describes 1) the collection of an extensive force dataset characterized by human-robot contact events, and 2) classification models informed by this dataset to determine the nature of the interaction. We demonstrate high classification accuracies among our proposed gesture definitions on a test set, emphasizing that neural network classifiers on the raw data outperform several other combinations of algorithms and feature sets.

## I. INTRODUCTION

### A. Motivation and Applications

An ultimate goal of the robotics sector of Human-Robot Interaction (HRI) is to enable interactions so natural and efficient as to reach parity with human-human interactions. Attainment of this lofty goal can be significantly advanced by improving a robotic system’s keen sense of touch, a sense which humans seamlessly and continuously use to perform any physical task.

### B. Prior Work

There are many works in the existing literature that make progress towards natural physical human-robot interactions. One such research area focuses on human-robot “handovers”, an event in which a giver transfers an object to a recipient. This is an interesting challenge in robotics because there is much to learn from human-human handovers, which have been characterized quantitatively [1], [2], [3]. Even nonverbal communication prior to the moment of handover contact has yielded its own study [4]. Such interactions can communicate beyond the physical, as handshakes have been shown to elicit affective state changes and theories of the personality of one’s handshake partner [5], [6], [7], with far-reaching consequences demonstrated in the field of haptics [8].

Elizabeth “Bibit” Bianchini is with the Department of Mechanical Engineering and Applied Mechanics, University of Pennsylvania, Philadelphia, PA 19104, bibit@seas.upenn.edu

Kenneth Salisbury is with the departments of Computer Science and Surgery, Stanford University, Stanford, CA 94305, jks@robotics.stanford.edu

Prateek Verma is an affiliate with the Artificial Intelligence Laboratory at the Department of Computer Science, Stanford University, Stanford, CA 94305, prateekv@stanford.edu

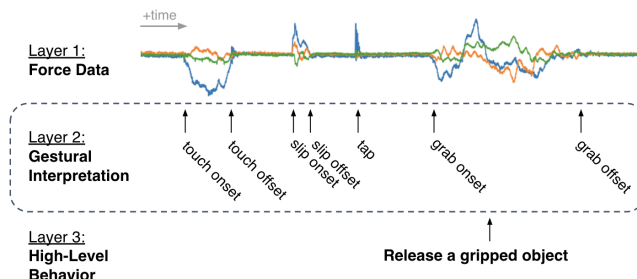


Fig. 1. This work aims to build a competent gestural interpretation layer, as illustrated above in relation to low-level force sensor data and to high-level behavioral system decisions. The above exemplifies the utility of this layer for the purpose of a robot-to-human object hand-off.

Currently there exists a dramatic disparity between the efficient, intuitive nature of human-human handovers and the often awkward, ill-informed nature of human-robot handovers. Simply grasping an object with acceptable grip forces is a challenging problem researchers have faced [9]. Some examples of HRI handovers require the human to apply aggressive forces for the robot to detect when to release a transferred object [10], and others implement thresholding of single parameters, such as jerk [11]. A different approach that results in markedly “human-like” HRI handovers requires a fixed, calibrated external camera [12], a reliance that cannot be feasibly implemented on mobile platforms or in dynamic and/or unknown environments.

The incorporation of machine learning tools to assist robotic systems with interpreting contact with their environments has led to more sophisticated improvements. Self-supervised learning methods on robotic systems with touch and vision capabilities can enable the robot to perform dexterous tasks such as inserting pegs in holes [13]. Convolutional Neural Networks (CNNs) can accurately quantify force values by interpreting other tactile sensor readings [14]. A particularly exciting work ports a classification algorithm trained on human-human handover forces onto a robotic platform, which uses the classifier to assist in performing HRI handovers [15]. They used energies of the output of the wavelet decomposition of the signal, as a feature representation of the force signals, followed by a linear classifier.

The existing literature surrounding human-robot contact presently demonstrates an extremely limited vocabulary of types of interactions, distinguishing only one type of human interaction [10], [11], [15]. We propose that an expanded definition set of human-robot contact events is a critical new direction to facilitate characteristically “human” physical interactions (thus, efficient and effortlessly smooth interactions) between robots and humans.

### C. Contributions and Paper Organization

In this paper, we demonstrate the development of a robotic system’s sense of touch by defining a tactile vocabulary of physical human contact gestures. We present the efficacy of classification models to interpret human contact events on the end effector from force sensor readings at the wrist.

Section II presents a vocabulary of gestural types to describe human-robot contact events and characterizes the dataset design and collection used for the remainder of this project. Section III describes the unique feature sets, and Section IV describes the algorithms explored in this paper. Section V presents the results of the trained models, using combinations of feature sets and algorithms aforementioned. We conclude in Section VI with suggested directions for future work.

## II. PROBLEM FORMULATION

### A. Gesture Definitions and Vocabulary

A dictionary of tactile gestures from human to robot was developed to differentiate between categories of human intent or preparedness. The four types of gestures outlined in this dictionary are 1) tap, 2) touch, 3) grab, and 4) slip. The distinctions among each of these gestures are outlined as follows:

1) *Tap Gesture*: A tap is characterized by an impulse-like event, wherein contact is made and broken in quick succession between the human and the robot.

2) *Touch Gesture*: A touch is similar to a tap gesture in that contact is made and broken between the human and the robot. The differentiating characteristic is that a touch can last for an indefinite duration, whereas taps typically appear as approximately 200 millisecond impulse-like events.

3) *Grab Gesture*: A grab is equivalent to more than one simultaneous touches from different directions. This subtlety between touches and grabs becomes critical in human-robot handovers, in which touches on their own may not effect capability of maintaining control of an object. The duration of a grab gesture, like that of a touch, can be indefinite.

4) *Slip Gesture*: A slip characteristically involves dynamic friction between the human and the robot. A slip may otherwise appear as a grab (contact from one primary direction) or as a touch (contact from two primary directions). The duration of a slip gesture is also indefinite.

These four categories are not comprehensive, as tactile interactions are analog in nature and can involve many other facets not encompassed by these definitions. For the purposes of these experiments, the four described gestures outline a vocabulary of distinct interactions that 1) could be intentionally used to communicate from human to robot, and 2) cover a broad scope of potential unorchestrated human-robot interactions in which these distinctions can encode critical information, resulting in whether a fragile object is successfully transferred or dropped, for example.

### B. State-Based and Transition-Based Approaches

A robotic system can keep track of occurrences of the four gestures throughout time series data in two ways: by identifying the current state (i.e. determining whether a gesture is currently happening and which gesture) or by identifying transitions between states (i.e. recognizing a change of gesture occurrence or type).

A system that implements a state-based tactile gesture identification model can infer the transition events, as can a transition-based model infer the current state. Thus, a system only has to implement one of these strategies accurately to effectively gain a sense of touch. The models developed in this paper pursued the state-based approach.

### C. Dataset Generation

Due to the lack of an existing dataset that covers our proposed range of tactile gestures, the data used in this project was collected in the Salisbury Robotics Lab, using a UR5e collaborative robotic arm. The built-in six-axis wrist force sensor and its design as a collaborative system renders the UR5e an attractive option for HRI applications in which a robot’s sense of force-based touch perception could elegantly offer extensive new capabilities.

The dataset used for training and testing the developed models is comprised of force readings of user subjects who were instructed to apply each of the four gesture types to the end effector of the robot (see Figure 2). The dataset represents 24 minutes of force sensor readings sampled at 500 Hz. The models described herein omitted the three torque channels, though future iterations could utilize these to possibly improve in performance. The raw data was filtered to remove noise, then cut into 600 millisecond duration overlapping snippets, generated at 100 millisecond increments. The chosen duration is long enough for entire taps to appear within a single snippet, while short enough for a robot to make reasonable real-time decisions.

## III. FEATURE SETS

This work analyzes the force sensor data to isolate and identify the presence and type of tactile interactions with a

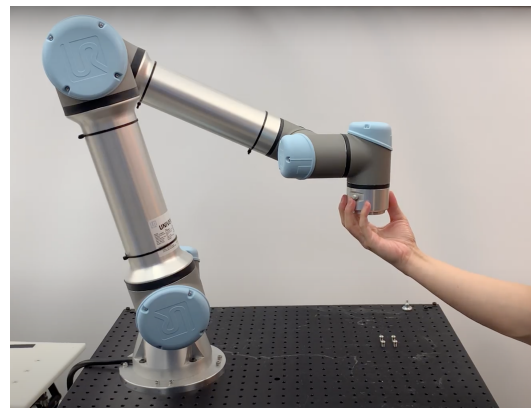


Fig. 2. An example of a user initiating a “grab” gesture to the robotic arm’s end effector during the data collection experiments.

human. Several feature sets were explored, including the full filtered data itself. The other five feature sets employed by some of these models intend to decrease the dimensionality. The permutations of feature sets and algorithms employed in this research are illustrated in Figure 3.

### A. Autoencoder Bottleneck

Two of the five reduced-size feature sets were generated using a reconstruction convolutional autoencoder model. These models learn a compressed version of the original snippet at the network’s bottleneck [16]. Manual verification determined the efficacy of these models by comparing their output vectors to their input vectors. Two feature sets were constructed in this way: one of 100 dimensions, and another of 60 dimensions, described by the size of the bottleneck features.

### B. Manual Feature Selection

The remaining three reduced-size feature sets were constructed manually based on distinguishing characteristics between the gestures in the force sensor readings (see Figure 4). These visuals provided insight into characteristics that could both unify different examples of the same gesture and discriminate from other gestures.

41 features were designed to capture some of these critical characteristics. Each of these features is designed to be invariant in the presence of a force offset. Prior to their usage in training the subsequent algorithms, each feature was normalized. The features are described in more detail below.

1) *Slope*: An obvious characteristic of the onset and offset of certain gestures is a sudden peak in first-order differences, which when coupled in quick succession, could additionally isolate tap events. Two features were generated by storing the most positive and most negative first-order difference across a window within the snippet’s three force channels. Mathematically, the maximum first-order difference feature  $f_1$  is calculated:

$$f_1 = \max(F_{n+w}^i - F_{n-w}^i) \quad (1)$$

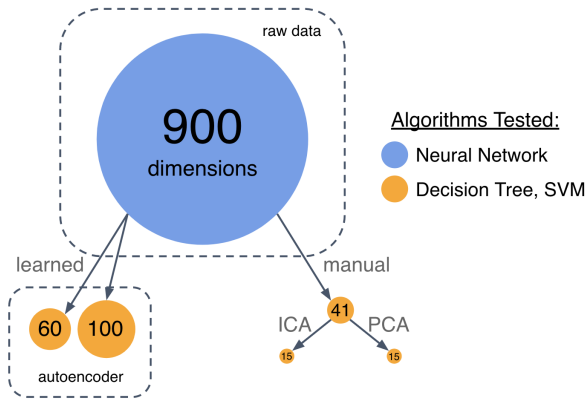


Fig. 3. Six feature sets and three classification algorithms were tested, for a total of 11 models. The above shows the feature sets’ relationships, relative dimensionality, and algorithm(s) employed on them.

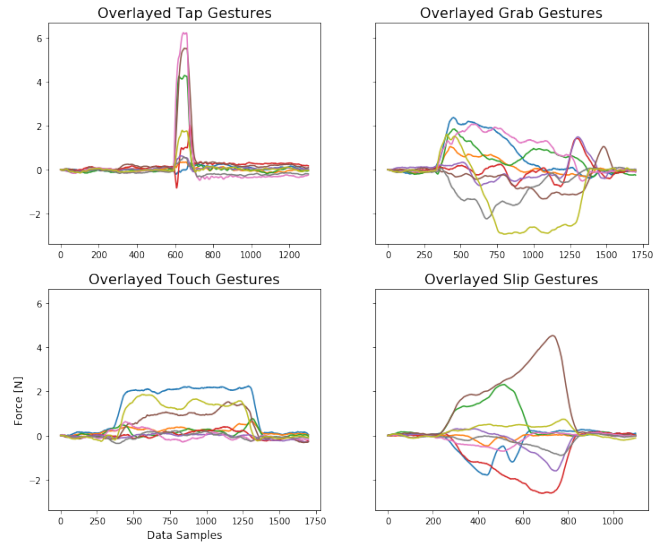


Fig. 4. The above plots illustrate groupings of each gesture type as they appear through force sensor readings. Each subplot displays several examples of like gesture types for similar durations of time.

where  $i = x, y, z$  are force data directions,  $w$  is half the window width in data points, and  $n$  is the data point number within the snippet with  $w \leq n \leq L - w$ , where  $L$  is the length of the snippet (300 data points). The window size  $2w$  was tuned based on the signal-to-noise ratio of the force sensor readings. Feature  $f_2$  is calculated similarly to obtain the steepest negative slope throughout the snippet. Additionally, average slopes for each channel throughout the snippet were stored as  $f_3, f_4,$  and  $f_5$ . Feature  $f_3$  exemplifies the  $x$ -direction:

$$f_3 = \frac{12}{L^3 - L} \cdot \sum_{k=1}^L \left[ \left( k - \frac{L+1}{2} \right) (F_k^x - F_{avg}^x) \right] \quad (2)$$

This expression is derived from the slope of the line of best fit using least squares error.

2) *Duration of High Slope*: A distinguishing feature of a grab gesture as opposed to a touch gesture is the wavering in the force magnitude throughout the contact. Because a grab intrinsically involves more than one direction of contact, the net force captured by the force sensor can unpredictably vary between opposing directions as the human applies uneven pressure through their grip. Features  $f_6, f_7, f_8$  aim to capture this characteristic by quantifying the number of data points in a row for each channel that exhibited absolute value first-order differences above a tuned threshold.

3) *Curvature*: Touch gestures appear to be more square in profile than grab or slip gestures. A metric to capture this quality is a sudden change in the slope of the force data, a characteristic that can be captured by a sharp change in adjacent calculations for first-order differences. The most positive and the most negative second-order differences were stored. First, a vector of first-order differences is calculated:

$$\mathbf{d}^i = [F_1^i - F_{2w+1}^i, F_2^i - F_{2w+2}^i, \dots, F_{L-2w}^i - F_L^i] \quad (3)$$

for  $i = x, y, z$  directions. Then:

$$f_7 = \max(d_{m+1}^i - d_m^i) \quad (4)$$

with  $0 \leq m \leq L-2w$ , the length of the  $d^i$  vector. Features  $f_7$  and  $f_8$  encode the peak (maximum and minimum) second-order differences. Again using least squares error, the average second-order slopes are additionally stored as  $f_9$ ,  $f_{10}$ , and  $f_{11}$ :

$$f_9 = \frac{12}{M} \cdot \sum_{k=1}^{L-2w} \left[ \left( k + w - \frac{L+1}{2} \right) (d_k^x - d_{avg}^x) \right] \quad (5)$$

for the  $x$ -direction, where  $M = L^3 - 6L^2w - 3L^2 + 24Lw^2 + 5L - 32w^3 + 2w - 3$ .

4) *Duration of High Curvature*: Feature  $f_{12}$  stores the number of data points in a row that exhibited absolute value second-order differences above a tuned threshold.

5) *Standard Deviation*: One possible way of detecting human contact is by calculating the standard deviation. During periods of no contact, the force sensor readings are less dynamic than when there is any form of human contact. Feature  $f_{13}$  takes the average standard deviation over all of the  $x$ ,  $y$ , and  $z$  directions:

$$f_{13} = \frac{1}{3} \sum_{i=x,y,z} \sqrt{\frac{1}{L-1} \sum_{k=1}^L (F_k^i - F_{avg}^i)^2} \quad (6)$$

6) *Third-Order Polynomial Fit*: A third-order polynomial approximation is constructed for each of the  $x$ ,  $y$ ,  $z$  channels. Of these polynomial coefficients, the cubic, quadratic, and linear terms were stored as features, excluding the constant terms. This yields three coefficients across the three channels for nine features,  $f_{14}$  through  $f_{22}$ .

7) *Tap Profile*: Tap gestures in particular share more common traits than any of the other gestures. Because the duration of a tap is consistently around 150-200 milliseconds, tap gestures all resemble a similar profile, albeit differing in direction and magnitude. An existing method that compares an input signal to a preselected template signal is called window main-lobe matching [17]. To implement, all snippet channel data are compared to a template tap profile. If the data points closely resemble the template, the resulting correlation error is low. Mathematically, a normalized correlation error  $\xi$  is given by:

$$\xi = \frac{\epsilon}{\sum_a^{a+b} X^2(k)} \quad (7)$$

$$\text{where } \epsilon = \sum_a^{a+b} [X(k) - |A|W(k)]^2 \quad (8)$$

$$\text{and } A = \frac{\sum_a^{a+b} X(k)W(k)}{\sum_a^{a+b} W^2(k)} \quad (9)$$

$\xi$  is a normalized form of the error  $\epsilon$  of an input signal  $X$  compared to a template signal  $W$ , selected from the template data.  $A$  is a scaling factor to ensure scale-independence, meaning a high force template tap could still be useful in detecting a tap of low force. Per snippet, two 320-millisecond templates – one for an upwards tap, one for a downwards tap – are compared against each of the force channels, and both the lowest and highest error  $\xi$  to each template are stored, yielding features  $f_{23}$ ,  $f_{24}$ ,  $f_{25}$ , and  $f_{26}$ .

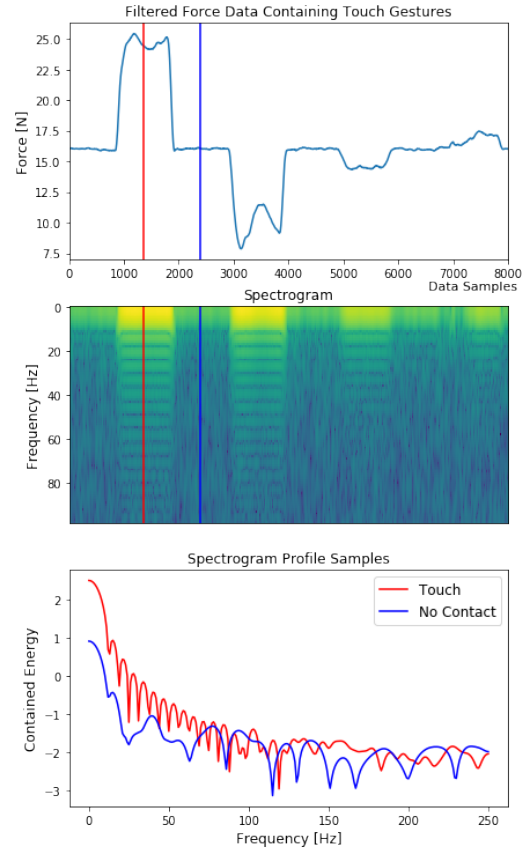


Fig. 5. Force sensor data (top) produces a spectrogram (center) that displays more energetic frequency content at low frequencies during touch events than during periods of no human contact. This is captured by a linear approximation for a time slice of the frequency content. Two example slice profiles are illustrated (bottom), with their corresponding time stamps marked in the upper two plots.

8) *Spectrogram Slice Linear Approximation*: Noting similarities between force sensor data and audio data, we employed many techniques commonly used for audio signal analysis [18]. One such technique is short-time Fourier transform, which quantifies the frequency content throughout a time series signal. Previous studies indicate that humans have particular tremor frequencies [19] that could be injected into a robotic system’s force sensor readings at the occurrence of human contact. Figure 5 demonstrates the ability of this tool to clearly distinguish contact events from non-contact events, the former of which exhibit higher energies of lower frequencies.

For each of the three channels and through time, a linear line with least squared error is computed for the spectrogram slice profile. Of these, the maximum, minimum, and average value for both the slope and offset are stored as features  $f_{27}$  through  $f_{32}$ .

9) *Spectral Rolloff, Centroid, and Flatness*: There are several other ways of characterizing frequency content from a generated spectrogram [20]. Among those are:

- Spectral rolloff: the frequency beyond which a diminishing proportion of the total energy is contained.
- Spectral centroid: a measure akin to the “center of mass” of the frequency content.

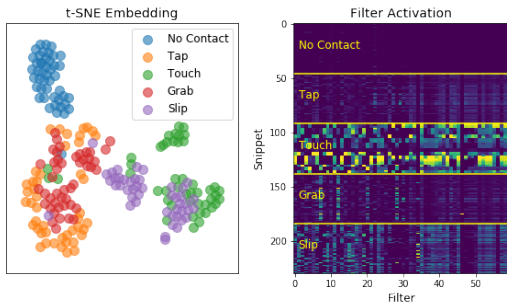


Fig. 6. A t-SNE plot (left) of a convolutional layer for the validation set indicates clustering of gesture types, and filter activations (right) throughout the CNN demonstrates similar activation patterns within like gesture types.

- Spectral flatness: a quantification of tone-like versus noise-like characteristics.

The remaining nine features,  $f_{33}$  through  $f_{41}$ , are the average values of spectral rolloff, spectral centroid, and spectral flatness across each of the three force data channels.

### C. Principal and Independent Component Analysis

Lower dimensional representations of the manually selected features  $f_1$  through  $f_{41}$  are also evaluated, via principal component analysis (PCA) and independent component analysis (ICA). Using PCA, 15 principal components are selected to maintain 95% of the training data variance at a reduced dimensionality. To match the PCA feature set size, 15 independent components are generated using ICA.

## IV. ALGORITHMS

### A. Models for Autoencoder Feature Sets

The autoencoders trained to generate the two learned feature sets discussed in Section III-A are CNNs [21], [22] built using Keras [23]. Both autoencoder models use 128 filters, optimized with the Adam optimizer [24] with a learning rate of  $1e-4$  over 1000 epochs with a batch size of 128, saving the weights corresponding to the lowest validation loss.

### B. Classifiers

This research evaluates three classifier algorithm types: decision trees, support vector machines (SVM), and neural network classifiers. While all three algorithms generally improve with larger datasets, the size of a sufficiently large dataset for neural network classifiers is particularly difficult to determine [25] and was not guaranteed to be met by our collected dataset.

A neural architecture search [26] was performed for the neural network model. The final model was determined through two selection rounds: the first round stored several models with the highest validation accuracy over 200 epochs with a batch size of 128, and a second round trained that limited set of models for an additional 1000 epochs at a 10x slower learning rate, saving the lowest validation loss thereafter. All optimization used the Adam optimizer [24]. The final model has 16 filters, an initial learning rate of  $1e-4$ , and 5 convolution layers, each followed by a dropout layer to mitigate overfitting [27], with dropout rates of 0.5 after the first 3 convolution layers and 0.1 after the last 2. We opted

for simple linear convolutions instead of dilated convolutions [28], as our force signal application has near-sighted contexts and does not require solving long-term dependencies, which dilated convolutions excel at modelling. Validation set t-SNE and filter activation plots are shown in Figure 6.

Hyperparameter searches were performed for each feature set on the decision tree and SVM algorithms. The hyperparameter combinations that yielded the highest validation set accuracy were selected. The Appendix contains more details on the iterated hyperparameters.

## V. RESULTS

The training set contains 319 snippets for each of the five states, totaling 1,595 examples. A validation set contains 46 snippets for each category, totaling 230 examples. The test set contains 27 snippets per category, for 135 examples.

The overall accuracy results are given in Table I, and a breakdown of true and false positives across all models and gesture types are plotted in Figure 7. Despite a small dataset, the best performing algorithm is the neural network classifier, which uses the force data directly as its feature set, obtaining a test set accuracy of 80.7%. The next best performance is 75.6% test accuracy, exemplified by the SVM algorithm with the autoencoder bottleneck feature set of dimension 100. These top neural network and SVM models perform markedly better than even the best decision tree model, which obtains 68.1% accuracy using the ICA feature set.

Confusion matrices for the top performing algorithms of each category (decision tree, SVM, neural network) are presented in Figure 8. These matrices indicate the weak points of each model. For example, the highest performing decision tree model’s accuracy is skewed upward because the confusion matrix (top in Figure 8) indicates this particular model seldom predicts touch gestures, inflating the likelihood of correctly guessing each of the other four categories. The model misclassified the majority of the actual touch gestures as grab gestures.

The neural network and SVM models displayed similar patterns of misidentification. For the neural network, approximately half of all touch gestures were misclassified, either as slip or grab gestures. Additionally, while still correctly classifying the majority of tap gestures, the neural network model incorrectly labeled a significant portion as no contact. Tap gestures had some of the highest recall in the training and validation sets, so this difference in the test

Feature Set	Decision Tree	SVM	NN
Manual	63.0%	65.9%	-
PCA	57.0%	67.4%	-
ICA	68.1%	68.1%	-
Autoencoder 60	67.4%	69.6%	-
Autoencoder 100	51.1%	75.6%	-
Force Data	-	-	80.7%

TABLE I

TEST SET ACCURACIES BY FEATURE SET AND ALGORITHM

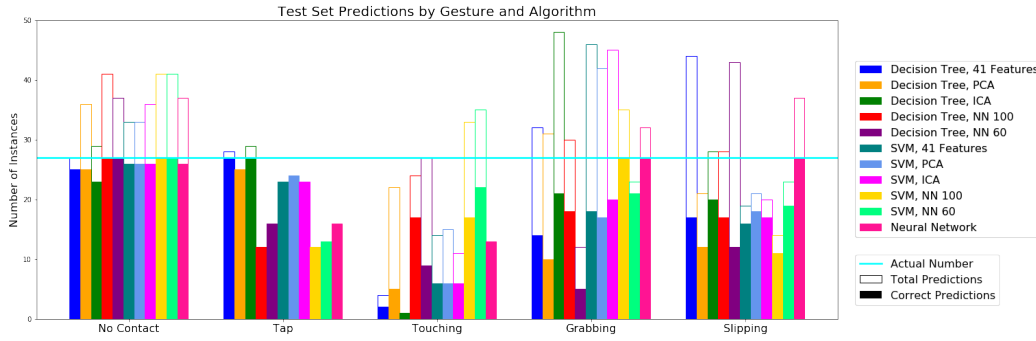


Fig. 7. This plot shows the true and false positives for each of the 11 trained classification models for each of the 5 state-based categories on the test set.

Decision Tree, ICA: Confusion Matrix

	Predicted No Contact	Predicted Full Tap	Predicted Touching	Predicted Grabbing	Predicted Slipping
Actual No Contact	23	0	0	3	1
Actual Full Tap	0	27	0	0	0
Actual Touching	4	0	1	19	3
Actual Grabbing	2	0	0	21	4
Actual Slipping	0	2	0	5	20

SVM, NN 100: Confusion Matrix

	Predicted No Contact	Predicted Full Tap	Predicted Touching	Predicted Grabbing	Predicted Slipping
Actual No Contact	27	0	0	0	0
Actual Full Tap	14	12	0	1	0
Actual Touching	0	0	17	7	3
Actual Grabbing	0	0	0	27	0
Actual Slipping	0	0	16	0	11

Neural Network: Confusion Matrix

	Predicted No Contact	Predicted Full Tap	Predicted Touching	Predicted Grabbing	Predicted Slipping
Actual No Contact	26	0	0	1	0
Actual Full Tap	11	16	0	0	0
Actual Touching	0	0	13	4	10
Actual Grabbing	0	0	0	27	0
Actual Slipping	0	0	0	0	27

Fig. 8. Confusion matrices for the top performing – by test set accuracy – decision tree algorithm (top), SVM algorithm (center), and neural network classifier.

set was unexpected. Further inspection indicated that several of the test set’s taps were particularly low in amplitude in comparison to the training examples.

## VI. FUTURE WORK

### A. Increase Accuracy and Robustness

Despite training on a dataset smaller than typical machine learning applications, this research demonstrates significant promise for employing tactile gestural identification models for robotic tasks. Techniques such as distillation [29] and data augmentation can improve performance using the existing dataset. These models can be made more robust by expanding the dataset [26], [30] through more human experiments. A larger dataset in concert with distillation

and/or data augmentation will likely improve the accuracy and generalizability of these developed models.

### B. Integrate Classifier with Goal-Oriented Tasks

The research goal is to integrate a gestural identification model in real-time on a robotic system to provide feedback in higher-level behavioral tasks. Such integration will require interpreting force sensor readings on a moving system.

### C. Active Exploration of Environment

The developed models so far identify tactile events inflicted by a human to a robot. There exists enormous opportunity for the robot to learn more about its environment and human contacts if it performs its own active exploration. For instance, a robotic arm could determine a measure of stability of a human’s grasp by actively quantifying the mechanical impedance the human imposes to the robot through the grasped object. Such a measure could be critical in human-robot handovers of fragile objects.

## VII. CONCLUSION

The developed classification models documented in this paper can effectively equip a robotic system with a sense of touch in HRI scenarios. This work demonstrates the capability to identify human tactile gestural events using only force sensor readings. Such capabilities can elegantly assist robotic systems in tasks with human collaborators, providing the robot with a translator for human’s natural gestural language.

## APPENDIX

The following are the hyperparameters varied during our searches for each algorithm-feature set combination. *Decision Tree*: max. tree depth, min. samples per leaf, min. samples per split, random state variable (for repeatability). *SVM*: regularization parameter, kernel type, kernel coefficient (for ‘rbf’, ‘poly’, and ‘sigmoid’ kernels), decision shape, random state variable. *Neural Network*: network topology, learning rate, filters, early layer dropout, late layer dropout.

## ACKNOWLEDGMENTS

This work was supported by the National Defense Science and Engineering Graduate Fellowship and in part by the Amazon Research Awards Program.

## REFERENCES

- [1] W. P. Chan, C. A. Parker, H. M. Van der Loos, and E. A. Croft, "Grip forces and load forces in handovers: Implications for designing human-robot handover controllers," in *Proceedings of the Seventh Annual ACM/IEEE International Conference on Human-Robot Interaction*, ser. HRI '12. New York, NY, USA: Association for Computing Machinery, 2012, p. 9–16. [Online]. Available: <https://doi-org.proxy.library.upenn.edu/10.1145/2157689.2157692>
- [2] K. Strabala, M. K. Lee, A. Dragan, J. Forlizzi, S. S. Srinivasa, M. Cakmak, and V. Micelli, "Toward seamless human-robot handovers," *J. Hum.-Robot Interact.*, vol. 2, no. 1, p. 112–132, Feb. 2013. [Online]. Available: <https://doi.org/10.5898/JHRI.2.1.Strabala>
- [3] A. H. Mason and C. L. MacKenzie, "Grip forces when passing an object to a partner," *Experimental Brain Research*, vol. 163, pp. 443–456, 2005.
- [4] M. K. Pan, V. Skjervøy, W. P. Chan, M. Inaba, and E. A. Croft, "Automated detection of handovers using kinematic features," *The International Journal of Robotics Research*, vol. 36, no. 5-7, pp. 721–738, 2017.
- [5] J. N. Bailenson, N. Y. Ph.D., S. B. Ph.D., D. Merget, and D. Koslow, "Virtual interpersonal touch: Expressing and recognizing emotions through haptic devices," *Human-Computer Interaction*, vol. 22, no. 3, pp. 325–353, 2007. [Online]. Available: <https://www.tandfonline.com/doi/abs/10.1080/07370020701493509>
- [6] J. N. Bailenson and N. Yee, "Virtual interpersonal touch and digital chameleons," *Journal of Nonverbal Behavior*, vol. 31, pp. 225–242, 2007. [Online]. Available: <https://doi.org/10.1007/s10919-007-0034-6>
- [7] F. Vigni, E. Knoop, D. Prattichizzo, and M. Malvezzi, "The role of closed-loop hand control in handshaking interactions," *IEEE Robotics and Automation Letters*, vol. 4, no. 2, pp. 878–885, 2019.
- [8] S. Brave, C. Nass, and E. Sirinian, "Force-feedback in computer-mediated communication," *Universal Access in HCI: Towards an Information Society for All*, vol. 3, 2001.
- [9] M. J. Sadigh and H. Ahmadi, "Safe grasping with multi-link fingers based on force sensing," in *2009 IEEE International Conference on Robotics and Biomimetics (ROBIO)*, 2009, pp. 1796–1802.
- [10] K. Nagata, Y. Oosaki, M. Kakikura, and H. Tsukune, "Delivery by hand between human and robot based on fingertip force-torque information," in *Proceedings. 1998 IEEE/RSJ International Conference on Intelligent Robots and Systems. Innovations in Theory, Practice and Applications (Cat. No.98CH36190)*, vol. 2, 1998, pp. 750–757.
- [11] J. Konstantinova, S. Krivic, A. Stilli, J. Piater, and K. Althofer, "Autonomous object handover using wrist tactile information," in *Towards Autonomous Robotic Systems*, Y. Gao, S. Fallah, Y. Jin, and C. Lekakou, Eds. Cham: Springer International Publishing, 2017, pp. 450–463.
- [12] M. Pan, E. Knoop, M. Backer, and G. Niemeyer, "Fast handovers with a robot character: Small sensorimotor delays improve perceived qualities," in *IEEE/RSJ International Conference on Intelligent Robots and Systems (IROS)*, 2019.
- [13] Y. Li, J.-Y. Zhu, R. Tedrake, and A. Torralba, "Connecting touch and vision via cross-modal prediction," in *Proceedings of the IEEE Conference on Computer Vision and Pattern Recognition*, 2019, pp. 10 609–10 618.
- [14] B. Sundaralingam, A. S. Lambert, A. Handa, B. Boots, T. Hermans, S. Birchfield, N. Ratliff, and D. Fox, "Robust learning of tactile force estimation through robot interaction," in *2019 International Conference on Robotics and Automation (ICRA)*, 2019, pp. 9035–9042.
- [15] W. He and D. Sidobre, "Improving human-robot object exchange by online force classification," 2015.
- [16] G. E. Hinton and R. R. Salakhutdinov, "Reducing the dimensionality of data with neural networks," *science*, vol. 313, no. 5786, pp. 504–507, 2006.
- [17] V. Rao, P. Gaddipati, and P. Rao, "Signal-driven window-length adaptation for sinusoid detection in polyphonic music," *IEEE Transactions on Audio, Speech, and Language Processing*, vol. 20, no. 1, pp. 342–348, 2012.
- [18] G. Peeters, "A large set of audio features for sound description (similarity and classification) in the cuidado project," *CUIDADO IST Project Report*, vol. 54, no. 0, pp. 1–25, 2004.
- [19] R. N. Stiles and J. E. Randall, "Mechanical factors in human tremor frequency," *Journal of Applied Physiology*, vol. 23, no. 3, pp. 324–330, 1967, PMID: 6047952. [Online]. Available: <https://doi.org/10.1152/jap.1967.23.3.324>
- [20] B. McFee, C. Raffel, D. Liang, D. P. Ellis, M. McVicar, E. Battenberg, and O. Nieto, "librosa: Audio and music signal analysis in python," in *Proceedings of the 14th python in science conference*, vol. 8, 2015, pp. 18–25.
- [21] S. Kiranyaz, O. Avci, O. Abdeljaber, T. Ince, M. Gabbouj, and D. J. Inman, "1d convolutional neural networks and applications: A survey," *arXiv preprint arXiv:1905.03554*, 2019.
- [22] O. Ronneberger, P. Fischer, and T. Brox, "U-net: Convolutional networks for biomedical image segmentation," in *International Conference on Medical image computing and computer-assisted intervention*. Springer, 2015, pp. 234–241.
- [23] A. Géron, *Hands-on machine learning with Scikit-Learn, Keras, and TensorFlow: Concepts, tools, and techniques to build intelligent systems*. O'Reilly Media, 2019.
- [24] D. P. Kingma and J. Ba, "Adam: A method for stochastic optimization," *arXiv preprint arXiv:1412.6980*, 2014.
- [25] J. G. A. Barbedo, "Impact of dataset size and variety on the effectiveness of deep learning and transfer learning for plant disease classification," *Computers and Electronics in Agriculture*, vol. 153, pp. 46 – 53, 2018. [Online]. Available: <http://www.sciencedirect.com/science/article/pii/S0168169918304617>
- [26] T. Elsken, J. H. Metzger, and F. Hutter, "Neural architecture search: A survey," *arXiv preprint arXiv:1808.05377*, 2018.
- [27] N. Srivastava, G. Hinton, A. Krizhevsky, I. Sutskever, and R. Salakhutdinov, "Dropout: a simple way to prevent neural networks from overfitting," *The journal of machine learning research*, vol. 15, no. 1, pp. 1929–1958, 2014.
- [28] M. A. Lee, Y. Zhu, K. Srinivasan, P. Shah, S. Savarese, L. Fei-Fei, A. Garg, and J. Bohg, "Making sense of vision and touch: Self-supervised learning of multimodal representations for contact-rich tasks," in *2019 International Conference on Robotics and Automation (ICRA)*. IEEE, 2019, pp. 8943–8950.
- [29] G. Hinton, O. Vinyals, and J. Dean, "Distilling the knowledge in a neural network," *arXiv preprint arXiv:1503.02531*, 2015.
- [30] D. Ellis and N. Morgan, "Size matters: An empirical study of neural network training for large vocabulary continuous speech recognition," in *1999 IEEE International Conference on Acoustics, Speech, and Signal Processing. Proceedings. ICASSP99 (Cat. No. 99CH36258)*, vol. 2. IEEE, 1999, pp. 1013–1016.